CROATICA CHEMICA ACTA CCACAA **64** (2) 253–268 (1991)

YU ISSN 0011-1643
UDC 541.1
CCA-1998 *Original Scientific Paper*

Potentials Originating from Point-like and Homogeneously Distributed Charges on Spherical Primary Particles of Aggregates

Mirko Mirnik

Laboratory of Physical Chemistry, Faculty of Science, University of Zagreb, Zagreb, Yugoslavia

Received October 29, 1990

The coulombic, Debye-Hückel and Gouy-Chapman potentials in the vicinity of a spheric colloidal particle, charged with eight elementary ionic point charges surrounded by the ionic cloud were calculated using the corresponding theoretical equations. The »potential *vs.* distance« from the sphere surface functions are represented graphically. The influence of the counter ion electrolyte concentration upon the thickness of the ionic cloud and the influence of the same thickness on the cited functions were calculated. The interrelation between the Debye-Hückel potentials and the coagulation rate constant was analyzed. The coagulation rate constant is recognized to be proportional to the difference between the brownian motion kinetic energy and the electrostatic repulsion energy of particles surrounded by the ionic cloud. Arguments for the inapplicability, in the colloid chemistry, of the homogeneous charge distribution double layer models based on Gouy-Chapman and Nernst potentials are described. All postulates of the proposed theories were deduced from experimental observations in the AgI colloidal system. An experiment illustrating the growth of primary stable particles and their subsequent coalescence and aggregation (clustering) is described in detail.

INTRODUCTION

During the formation of many sols or coagulating suspensions, growing aggregates (AGGs) are formed. They are of very irregular form and size. Each of the AGGs consists, at a given coagulation time, of a given number, P, of primary particles (PPAs) while the space between them is filled up with the intermicellar electrolyte. A certain number of adsorbed ions or chemically bound ionogenic radicals are fixed to each PPA (*e.g.* I^- on AgI, citrate ion on Au, H^+ on hematite, $-CO_2^-$ on latex). The scatter of the size and form of PPAs is occasionally small. In some sols, on the smallest stable particles (PPSs), only one ion is adsorbed.[1,2] In AGGs, the PPAs are bigger than PPSs, and several ions or ionogenic radicals are fixed on each. Consequently, we consider it

worthwhile to analyze, as an example, the spheric model of PPA with 8 point charges fixed on the surface, although 4, 6, 10 or 12 are also possible. The known potentials arising in the vicinity of ionic charges are the electrostatic or coulombic potential, ψ_c, the ionic cloud potential, ψ_{ic}, and the Debye-Hückel potential, ψ_{DH}, as they are derived by the generally accepted Debye-Hückel theory. The sums of the potentials ψ_c, ψ_{DH}, ψ_{ic} resulting from the adsorbed »PDI-counter ion (CI)« electrolyte on a PPA will be calculated as a function of the distance from the surface in accordance with the law of superposition of potentials. It will be demonstrated that the difference »kinetic energy – DH electrostatic work« of two particles in collision is responsible for the stability and the coagulation rate constant.

To initiate a polemic discussion, the Gouy-Chapman potential, ψ_{GCH}, arising in the vicinity of the same PPA on which the same number or charges is homogeneously distributed on the surface, will be considered, as well as the coulombic potential, ψ_h, arising in the vicinity of the same PPA if no counter ions are assumed to be present but caused by the same number of charges homogeneously distributed on the surface.[3-12] Since the experimental evidence and some theoretical arguments suggest that in some sols eight elementary ion charges are fixed on each PPA, the spheric model with eight point charges symmetrically placed in the sphere surface will be analyzed. The values ψ_c was calculated for the flat plate model of discrete point charges.[13]

The point charge model serves well for the explanation of electrolyte properties by the elementary version of the Debye-Hückel theory. *E.g.*, the limiting law of the activity coefficients was elaborated by it. Analogously, the present point charge model of colloidal particles will serve in the same manner to explain the properties of colloidal particles. The distance of the closest approach of the ions was introduced for calculations of exact activity coefficients in higher, $10^{-3} < c$, electrolyte concentrations.

THEORETICAL

The Debye-Hückel and Gouy-Chapman Equations

First, the basic equations of the fundamental Debye-Hückel and Gouy-Chapman theories, as used in the present paper, are cited.

The variation of ψ_c with the distance, x/κ_o, from a single point charge, $z\,e_o$, can be defined by Coulomb's equation which reads:

$$\psi_C = ze_o\kappa_o/4\pi\varepsilon x \tag{1}$$

where $1/\kappa_o$ is the unit of distance and x its numerical value. The same equation can also be written in the form:

$$\psi_C/\psi_o = 1/x \tag{2}$$

where for $x = 1$:

$$\psi_o = ze_o\kappa_o/4\pi\varepsilon \tag{3}$$

can be considered a relative unit of potential and explained as the electrostatic potential at a distance $1/\kappa_o$ from the point charge $z\,e_o$ when the counter ion (CI) concentration is c ($z_+ = z_- = 1$) = $c_o = I$ (in equation 12)*.

The charge number is z, e_o the elementary charge, ε the permittivity of the medium.

The variation of the potential, ψ_h, caused by the same charge but homogeneously distributed on a sphere of radius r_s/κ_o, can be defined by:

$$\frac{\psi_h}{\psi_o} = \frac{1}{r_s + x} \tag{4}$$

It is equal to the potential which would exhibit the point charge $z\, e_o$ at a distance $(r_s + x)/\kappa_o$ from it.

The Debye-Hückel potential, ψ_{DH} (c_o,κ_o), or volume charge density, ρ, of a reference or central point charge is by the elementary Debye-Hückel theory defined by:

$$\psi_{DH}/\psi_o = \rho/\rho_o = e^{-x}/x \tag{5}$$

Here is $\rho_o(x=1) = z\, e_o\, \kappa_o^2/4\pi\, \varepsilon$

Their difference is the ionic cloud potential, Ψ_{ic}, and it is defined by:

$$\psi_{ic}/\psi_o = (\psi_{DH} - \psi_c)/\psi_o = (e^{-x} - 1)/x \tag{6}$$

The ionic cloud exhibits upon the central ion the potential $\psi_{ic,x \to o}$ which is defined by:

$$\psi_{ic,x\to o} = -\psi_o \tag{7}$$

This means that $\psi_{ic,x\to o}$ is equal in magnitude but of opposite sign to ψ_o.**

The radial charge density, ρ_r, is defined by:

$$\rho_r/\rho_{ro} = x\, e^{-x} \tag{8}$$

where $\rho_{ro}(x=1) = -z\, e_o\, 4\kappa_o\pi/e$. It represents the charge per unit surface of the sphere of radius $\kappa^{-1}{}_o$. The probability to find the CI at distance x from the central ion is ρ_r.

Analogously, the Gouy-Chapman potential, ψ_{GCH}, can be defined by:

$$\psi_{GCh}/\psi_o = -e^{-x}/[(r_s+x)r_s\, 4\pi] \tag{9}$$

because $\rho_i(x=1) = z\, e_o\kappa^o/4\pi\, r_s^2$ is the surface charge density. It is negative if the homogeneously distributed inner charge in the sphere surface is a deficit of electrons and positive if the inner charge is an excess of electrons. If one assumes that the »inner charge – diffuse charge« can be replaced by a capacitor of unit surface area of two thin layers of charges separated for the distance κ_o^{-1}, then the potential difference between the two layer is $\rho_o\kappa_o^{-1}/4\pi\, \varepsilon$ and is equal to ψ_{GCH}.

---

* Throughout this paper the numerical values of concentrations c or [symbol], should be multiplied by the unit »mol dm^{-3}«.

** Note: $e^{-x} = 1 - x + x^2/2! - x^3/3! \pm \ldots$, $e^{-x}(x=0) = 1$; $e^{-x}/x = 1/x - 1 + x/2! - x^2/3! \pm \ldots$, $(e^{-x} - 1)/x = -1 + x/2! - x^2/3! \pm \ldots$; $(e^{-x} - 1)/x\,(x = 0) = -1$

The potential exhibited by the ionic cloud upon the inner charge at $x = 0$ is, therefore, defined by:

$$\psi_{GCh,x\to 0} = -\psi_o/4\, r_s^2\pi \tag{10}$$

In the Debye-Hückel theory, as well as in the Gouy-Chapman theory, the parameter κ_o is defined by:

$$\kappa_o^2 = 2\, e_o^2 L/\varepsilon\, kTI \tag{11}$$

where the ionic strength, I, is defined by:

$$I = \frac{1}{2}\sum_i c_i z_i^2 \tag{12}$$

and c_i is the concentration, z_i the charge number of ions i present in the bulk electrolyte [for $z_+ = z_- = 1$, $c_o(1-1) = I$]. The Avogadro-Loschmidt constant is L.

Growth of Stable Primary Particles (PPSs) and the Formation of Primary Particles (PPAs) Forming Aggregates (AGGs)

A systematic experimental study of the growth of PPAs *via* coalescence and coagulation from PPSs was described earlier.[2,19] The growth of PPSs was evidenced by the increase of the intensity of scattered light (ISL) and by electronmicrography.[20] A typical selected experiment will be described in Figure 1.

To a solution [NaI] (starting) $= 1 \cdot 10^{-3}$, $pI_s = 3$, in small portions an $AgNO_3$ solution was added and $pI = -\log[I^-]$ was measured potentiometrically with a suitable »$Ag/Ag_2S,I^-$ reference electrode« cell as well as the parameter $\gamma = [I^-_{ads}]/[AgI]$. The more suitable variable was calculated by $\Delta pAg = pI^o - pI$ (pI^o is the value when $\gamma = 0$). The plots:

$$\gamma = \Gamma_o \Delta pAg \tag{13}$$

are linear with an abrupt change Γ_o at $pI = pAg - 8 = 8 = -\log\sqrt{K(AgI)}$; $K(AgI) = 10^{-16}$ is the ionic product of AgI.

Some characteristic values used for the construction of Figure 1 are:

slope: $\Gamma_o = 3 \times 10^{-3}$						slope: $\Gamma_o = 1.75 \times 10^{-3}$			
pI	3^x	3.63	5^x	8^x	9.4	8^x	9.4	10.31^x	10.4^x
ΔpAg	6.4	6.22	4.4	1.4	0	2.4	1	0.09	0
$\gamma 10^3$	19	18.65	13.2^x	4.2^x	0^x	4.2^x	1.75^x	0.1575^x	0^x
$1/\gamma$	0	53.6	75.8	238	∞	238	571	6345	∞
r_s/n	0	0.971	1.06	1.55	∞	1.55	2.07	4.62	∞

The values marked ^{x} were directly measured or obtained by linear extrapolation . The ionic strength, I, is constant because a part of NaI transforms into $NaNO_3$, $[I^-] + AgNO_3 = AgI$ (solid) + $[NO^-_3]$, $I = [NaI]_s = c_o(1-1) = 1 \times 10^{-3}$. Consequently, the DH–radius is $\kappa^{-1}{}_o = 9.24$ nm and $\psi^o{}_{DH}$ $(x=1) = -\psi_o$.

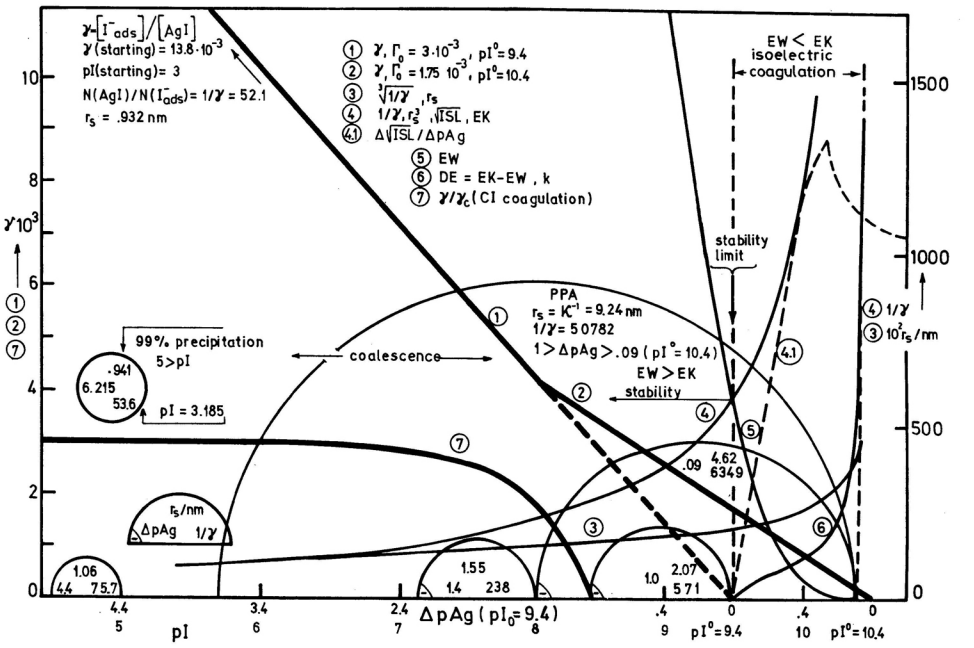

Figure 1. Precipitation and coalescence of stable primary particles (PPSs) during titration of [NaI] starting = $1 \cdot 10^{-3}$, $pI_s = 3$ with a $AgNO_3$ solution. Abscissa: pI and ΔpAg. Ordinate: $\gamma = [I^-_{ads}]/[AgI]$, $[AgI] = 10^{-pI_s} - 10^{-pI}$. Plots:(1) $\gamma, \Gamma_0 = 3 \cdot 10^{-3}$, $pI^\circ = 9.4$; (2) $\gamma, \Gamma_0 = 1.75 \cdot 10^{-3}$, $pI^\circ = 10.4$; (3) $\sqrt[3]{1/\gamma}$, r_s; (4) $1/\gamma$, r_s^3, $\sqrt[2]{ISL}$ = square scattered light intensity; *EK* = kinetic energy of PPSs; (4.1) $\Delta\sqrt{ISL}/\Delta pAg$; (5) *EW* = electrostatic work of PPS; *k* = coalescence + coagulation rate constant; (6) $DE = EK - EW, k/k^\circ$; (7) γ/γ_c(CI coagulation). Semicircles with inscribed values: ΔpAg, r_s/nm, $1/\gamma$. Range: $pI_s = 3 < pI < 9.4$ = stability limit, precipitation + coalescence; $9.4 < pI < 10.31$, r_s(PPS) < $k_0^{-1}/2$, coalescence + coagulation, r_s(PPA) = $\kappa^{-1}{}_0$ = 9.24 nm, $1/\gamma$ = 50782.

In Figure 1, the PPSs are visualized by semicircles of r_s (ΔpAg) of which the points opposite to the charge are at the value ΔpAg (or pI) of the abscissa, r_s is the radius of PPSs.

The PPSs formed in this way are the smallest possible and also their charge is the smallest possible, *i.e.* 1 I^-_{ads}. Their radius, r_s, can be calculated by (plot(3)):

$$r_s = \sqrt[3]{3\,MW/(4\pi\gamma L d)} \tag{14}$$

Here $MW = 235$ is the molar mass of AgI and $d = 6$ g cm^{-3} is the density. The plot (4) is identical for $1/\gamma$, r^3_s, $\sqrt{ISL}$, *EK* with a proper choice of ordinate unit values. According to the Raileigh theory, *ISL* (pI) is proportional to the second power of volume of the scattering particles. This means that $\sqrt{ISL} = K' r^3_s = K''/\gamma$. In the range $10^{-4} < [AgI] < 10^{-2}$, the experimental *ISL*(pI) and $\sqrt{ISL}$(pI) plots have an inflection. The intersection of the tangent through the inflection with the pI abscissa was termed

the »negative stability limit« (pI_{limit}). In the range $pI_s < pI < pI_{limit} = 9.4$, the sols are stable: over hours or even days the *ISL* remains constant or changes very slowly. In the range $9.4 < pI < 10.31$, *ISL* increases with time. By a proper choice of the $\sqrt{ISL}$ unit, the tangent through the inflection can be matched with tangent 4.1 on plot 4. At $\Delta pAg < 0.09$ ($pI = 10.31$) immediately after the last addition of Ag^+, the coagulation rate becomes inmeasurably big. In the sol, visible flocks are formed immediately and *ISL* decreases even prior to sedimentation. The supernatant electrolyte is clear after sedimentation of a few minutes.

The Primary Particle (PPA) Prior to the Start of Coagulation

If eight equal point charges, $z\,e_o$, are placed symmetrically on the sphere surface of radius r_s, then they are in the corners of a cube circumscribed by the sphere. If the corners of the cube are designated by J = A,B,C,D,E,F,G,H, then the coordinates of points x_J, y_J, z_J are:

J→	A	B	C	D	E	F	G	H
x_J→	$-r_s$	r_s	$r_s/3$	$-r_s/3$	$-r_s/3$	$-r_s/3$	$r_s/3$	$r_s/3$
y_J→	0	0	h	$h/2$	$h/2$	$-h$	$-h/2$	$-h/2$
z_J→	0	0	0	$h/2$	$-h/2$	0	$h/2$	$-h/2$

Here, $h = 2\,r_s\sqrt{2}/3$.

Three corners of the cube A, B, C and half of the cross-section of the sphere are shown in Figure 2. The numerical value of the radius of the sphere is $\overline{OA}$, $\overline{OB}$, $\overline{OC} = r_s$, one side of the cube is $\overline{BC}$, the diagonal of the plane is $\overline{AC}$. In total, in the cube there are 8 axes of the type O-A →, 6 of the type O-$\overline{BC}/2$ →, 6 of the type O-$\overline{AC}/2$ →. The slopes of the axes are $T_A = 0$, $T_{AC} = \sqrt{2}$, $T_{BC} = \sqrt{2}/2$.

The coordinates of the points on the three different axes are $yy = xxT_A$, $yy = xxT_{AB}$, $yy = xxT_{BC}$, $zz = 0$ where xx are preset values. The relative distance of a point on the axis from the centre 0 is rr and can be calculated by:

$$rr = \sqrt{xx^2 + yy^2} \tag{15}$$

The distance, r_J, from a charge J to a point on the axes can be calculated by:

$$r_j = \sqrt{(xx - x_j)^2 + (yy - y_j)^2 + z_j^2} \tag{16}$$

The relative distance, from the sphere surface to a point on an axis is:

$$x = rr - r_s \tag{17}$$

The total coulombic potential, ψ_{cs}, exhibited by the 8 point charges on a point on an axis is defined by:

$$\psi_{cs}/\psi_o = \sum_{J=A}^{H} 1/r_J \tag{18}$$

The analogous Debye-Hückel potential of the 8 charges, ψ_{DHS}, is defined by:

$$\psi_{DHS}/\psi_o = \sum_{J=A}^{H} \exp(-r_J)/r_J \tag{19}$$

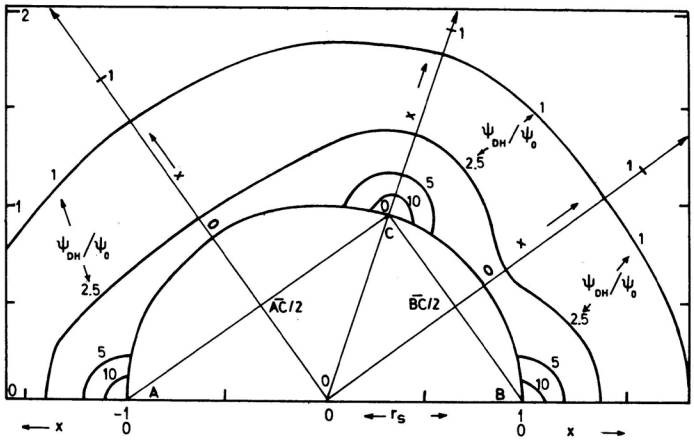

Figure 2. Half of the cross-section of the sphere of relative radius $r_s = 1$ with three point charges A, B, C in the corners of the inscribed cube. The axes across the centre are O-A→, O-B→, O-AC/2→, O-BC/2→. Cross-section of Debye-Hückel equipotential surfaces in the plane A–B–C for $\psi_{DH}/\psi_o = 1, 2.5, 5, 10$.

The coulombic potential of the 8 charges, ψ_h, though homogeneously distributed on the sphere surface, is in any direction defined by:

$$\psi_h/\psi_o = 8/(r_s + x) \tag{20}$$

It is equal to the potential which would exhibit a point charge $8\,z\,e_o$ in the centre 0 on a point at the distance $r_s + x$.

The ionic cloud potential of the 8 I^-_{ads} can be calculated by:

$$\psi_{ics} = \sum_{J=A}^{H} \psi_{DHs} - \psi_{cs} = \psi_o \sum_{J=A}^{H} \exp(-r_J - 1)/r_J \tag{21}$$

and it is for $x \to 0$ or $rr \to r_s$

$$\psi_{ics}(x \to 0) \approx \psi_o\, 3/4 \tag{22}$$

at the origin of all three axes.

The radial charge density function is defined by:

$$\rho_{rs}/\rho_o = \sum_{J=A}^{H} r_J\, e^{-r_J} \tag{23}$$

It represents the probability to find the CIs at distance x from the surface.

The Gouy-Chapman potential, ψ_{GCh}, if the 8 positive charges are homogeneously distributed on the sphere surface, is defined by:

$$\frac{\psi_{GChs}}{\psi_o} = \frac{2\,e^{-x}}{(r_s + x)\,r_s\pi} \tag{24}$$

The latter corresponds to the potential ψ_{ics}. Consequently, at $x=0$, the same potential is $\psi_{GCHs}(x=0)/\psi_o = -2\kappa_o^2/r_s^2\pi$.

In the calculation of the potentials ψ_{Cs}, ψ_{DHs}, ψ_{Hs}, ψ_{ics}, ψ_{GChs}, the influence of the permittivity of the PPA was neglected, because it is irrelevant for the present discussion.

Figure 3 shows the variation of the potentials ψ_{DHs}/ψ^o, and ψ_{cs}/ψ^o, ψ_{ics}/ψ^o and ρ_s/ρ^o with the distance, x, from the sphere surface along the three axes and the variation of the potential ψ_{GChs}. The variation of the potential ψ_h/ψ_o practically coincides with that of ψ_c/ψ_o along the axis O-$\overline{AC}/2$ → and for this reason it was not drawn.

The plots ψ_{cs} and ψ_{DHs} along the three axes are very different in contrast to the plots ψ_{ics} which, even for $x \to 0$, differ by less than 0.5% at the origin of the axes.

The plots ρ_{rs} differ in the vicinity of the surface along the three axes by a few percent only. Also, ψ_{ics} (PPA, $x \to 0$) = $\psi_o 3/4$. Consequently, the equipotential surfaces are practically concentric spheres for the latter two functions.

The reduction of $\psi_{ic,x\to o}$(PPS) = $-\psi_o$ to $\psi_{ics,x\to o}$(PPA) = $-\psi_o 3/4$ explains why 8 PPSs, each with 1 I^-_{ads}, coalesce to form 1 PPA with 8 I^-_{ads}. One big PPA ($r_s = \kappa^{-1}$) is at a lower energy level than the 8 PPSs ($r_s = \kappa^{-1}/2$) because the repelling forces between the charges are lower. This is the first argument for $A = 8\,e_o$ charges on 1 PPA.

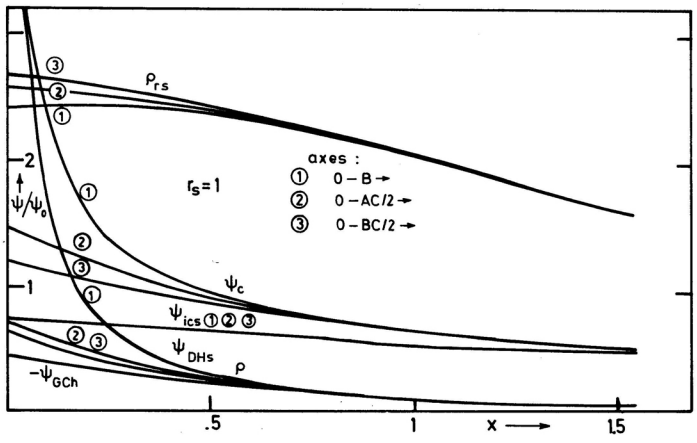

Figure 3. Dependence of Coulombic, ψ_c/ψ_o, Debye-Hückel, ψ_{DH}/ψ^o, ionic cloud, $-\psi_{ic}/\psi^o$, potentials, of radial charge density, ρ_r/ρ_{ro} along the axes O–B→, O–AC/2→, O–BC/2→ and the Gouy-Chapman potential, $-\psi_{GCh}/\psi_o$ of the relative distance, x, from the sphere surface.

If, due to the kinetic energy of the brownian notion, two PPSs approach each other, so that the distance between the charges will be maximum, or that ψ_{DHs}, $x = 2r_s$ in collision will be minimum, the two PPSs will orient themselves in the direction of the axes O-BC/2 → . Then, the repulsion is minimum.

The distance of the closest approach between CI and I^-_{ads} is of importance only for ψ_{Cs} and ψ_{DHs} at the origin of the axes O-B → . ψ_{Cs} and ψ_{DHs} are of negligible influence upon the collision energy along the axis O-BC/2 → .

If two PPSs of r_s charged with a single charge I^-_{ads} surrounded by the ionic cloud approach at the brownian motion velocity, their kinetic energy, *EK*, is determined also by their mass or volume:

$$EK/EK^o = r_s^3 \tag{25}$$

and EK^o is determined by the unit chosen for r_s(plot (4)) and for *EK*.

The Debye-Hückel energy, E_{DH}, of the two particles at each moment separated for the distance x between the two charges, can be defined by:

$$\frac{E_{DH}}{E^o_{DH}} = \rho_r^{(x/2)}\,\psi_{DH}^{(x/2)} = \frac{(x/2)e^{-x/2}\,e^{-x/2}}{(x/2)} = e^{-x} \tag{26}$$

where $E^o_{DH} = \rho^o_r\psi^o_{DH}$ for $x = 0$. The PPSs will meet in $x/2r_s$.

The electrostatic work, *EW*, to bring the two PPSs to collision, *i.e.* from the distance $x = n\,r_s$ to $2r_s$ can be defined by (plot 5):

$$EW/E^o_{DH} = \int_{x=nr_s}^{2r_s} \rho_r(x/2)\,\psi_{DH}(x/2)\,dx = \int_{x=nr_s}^{2r_s} e^{-x}\,dx = -e^{-x}\Big|_{nr_s}^{2r_s} \tag{27}$$

Since $n >> 2$ is determined by the number concentration of PPSs, $e^{-nr_s} = 0$. In collision, the distance between the point of collision and each charge is $2\,r_s$: Then:

$$EW/EW^o = exp(-2r_s) \tag{28}$$

If the difference

$$DE = EK/EK^o - EW/EW^o \tag{29}$$

is negative, prior to collision the PPAs will repel each other, if it is positive they will collide efficiently and coalesce. When their radius after repeated efficient collisions becomes $r_s = \kappa^{-1}{}_o/2 = 4.62$ nm and $1/\gamma = 6349$, they coalesce again and eight PPSs of $r_s = \kappa^{-1}{}_o/2$ produce one PPA of $r_s = \kappa^{-1} = 9.24$ nm, $1/\gamma = 50792$. These PPAs are in a state ready for coagulation. The overall coalescence and coagulation rate constant, k, is proportional to *DKE* [plot (6)].

When after a small addition of Ag^+, the value is close to $\Delta pAg = 0.09$, $\gamma \to 0$ and $1/\gamma \to \infty$, many PPAs lose their I^-_{ads}. Immediately after the last addition of Ag^+, r_s(PPS) = 4.62 nm = $\kappa^{-1}{}_o/2$ and $1/\gamma = 6349$ and immediately 8 PPSs coalesce to form 1 PPA of $r_s = \kappa^{-1}{}_o = 9.24$ nm and of $1/\gamma = 50792$. Many now PPAs of $r_s = \kappa^{-1}{}_o$ form visible

flocks. This momentaneous and visible flocculation served in Gay-Lussac volumetric determination of halogen ion as the equivalence or end point.

Momentaneous flocculation is a process with a very big rate constant or an extremely short halflife that were not measurable by the so far used methods of colloid chemistry.

Obviously, at the transition of the $\Delta pAg_{limit} = 1 \rightarrow (pI_{limit} = 9.4)$ $EK < EW$ changes into $EK > EW$, or the sign of DE changes. The coagulation rate constant becomes $k > 0$ or the stable systems become unstable due to »isoelectric« coagulation.

The definition of EW (equation 27) is not the only possible one for the brownian motion energy of PPSs surrounded by ionic cloud. The following products are also possible: $\rho(2r_s).\psi_{DH}(x-2r_s)$, $\rho_r(2r_s).\ \psi_{DH}(x-2r_s)$, $\rho(2r_s).\psi_{DH}(x-2r_s)$, $\rho(x/2).\psi_{DH}(x/2)$.

Their integration is more complicated but the resulting EW definitions are similar and the condition $EW = EK$ can be defined in an analogous way.

Formation of Primary Particles in the Presence of Counter Ions

If a solution of $2.2 \cdot 10^{-4} < [NaI] < 2.02 \times 10^{-2}$ is mixed with an equal volume of $[AgNO_3] = 2 \cdot 10^{-4}$, the resulting sol concentration is $[AgI] = 1 \cdot 10^{-4}$ and the ionic strength is $1 \cdot 10^{-4} < I = [NaNO_3] + [NaI]$ (excess) $< 1 \cdot 10^{-2}$ and $2 < pI < 5$. The sol is stable, *i.e.* no increase of the intensity of scattered light, *ISL*, can be observed for hours or even days. No coagulation occurs. If to such sols either $0.02 < [Na^+]$, or $3 \cdot 10^{-4} < 2.\ [Ba^{2+}]$, or $1 \cdot 10^{-5} < 3\ [La^{3+}]$, are added, after the addition the sols start to coagulate: *ISL* increases, the halflife of the process is about 10 minutes or more and it decreases with increasing $z[Me^{z+}]$. After about 1 hour the sol particles sediment, the overnatant electrolyte is clear.

The adsorption isotherm can be represented by:

$$\gamma/\gamma_c = 1 - 10^{-\Delta pAg} \quad \text{or} \quad (\gamma_c - \gamma)/\gamma_c = 10^{-\Delta pAg} \tag{30}$$

The maximum $\gamma = \gamma_c\ 10^{\log I/c}$ is the saturation value because for $\Delta pAg > 1$ and $\log I/c << 1$ is $1 > \gamma/\gamma_c > 0.9$.

In $c_{min} < c < c_c$, prior to the start of coagulation $r^3_s < \kappa_O^{-3/2} \propto 1/\gamma_s$, when the coagulation is finished $r^3_s = (\kappa_o 2)^{-3} \propto 1/\gamma_c$. As a consequence, $\gamma_s/\gamma_c = \Gamma^o_s/\Gamma^o_c = 2^3 = 8$. Figure 6 is the experimental confirmation of this postulate: $\Gamma^o_s = 3 \cdot 10^{-3}$, $\Gamma^o_c = 0.4 \cdot 10^{-3}$, $\Gamma^o_s/\Gamma^o_c = 3/0.4 = 8$ (2^{nd} argument of A=8).

Coagulation can set in when $k/k^o_c = DE/EK^o - EW/EW^o > 0$, *i.e.* when $c_{min} < c < c_c = ccc$.

During coagulation, the amount of AgI per PPA remains constant and is determined by r_s (PPA) $= \kappa^{-1}_o = 9.24$ nm, *i.e.* $1/\gamma$ (PPA) $= 50792 =$ const. Experimentally, [plot (7)] was determined $\gamma_c = 3 \cdot 10^{-3}$ and then the amount of AgI is bound to $1/I^-_{ads}$, $P = [1/\gamma(PPA)]/(1/\gamma_c) = 152$. The same P represents the number size of coagulated AGGs[21] after 3–4 coagulation halflifes.

The plots $\gamma_c(z)$ or $\Gamma^o_c(z)$ are parallel lines. Their shift can be expressed by the linear Schulze-Hardy rule:

$$\gamma_c(z) = \log [Me^o] - z\,SH \tag{31}$$

Its proportionality constant is SH (= 1.65 for AgI). The constant log [Me°] can be obtained by extrapolation of the $\gamma_c(z)$ values to $z=0$.

It was reported in the literature[14] (Figure 12, p. 320)[12] that the following linear relation between the stability factor, W and the coagulator concentration, $c = z$ [Me^z] is valid:

$$\log(W/W_c) = A \log(c/c_c) \tag{32}$$

where c_c is the critical coagulation concentration (*ccc*), W_c the corresponding stability factor and A is slope or the proportionality constant.[12]

The stability factor is defined by:

$$\log(W/W_c) = \log(k/k_c) \tag{33}$$

and k, k_c is the coagulation rate constant in c, c_c.

Experimentally, three regions of CI concentrations, c, can be distinguished: (I) the region $c < c$(aging) where the coagulation rate constant $k < k_a$ is smaller than the rate constant, k_a, of aging. If in this region, $c < c_a$(aging), a coarsening of the sol particles is observed, then it is not caused by coagulation but by crystal growth. The single particles are crystallites, while AGGs in coagulating sols are spongy structures of many PPAs. The space between them is filled up with electrolyte. (II) the region c(aging) < $c < c_0$ where the plot(32) is linear with the slope A. (III) the region $c_c < c$ where the plot(32) is constant.

The slope A was explained[21] as the number of Me$^z/z$ charges reacting with a single PPA according to:

$$z\,A\,I^-_{ads} + AMe^z_{bulk} = A\,(I^-_z\ Me^z)_{ads} \tag{34}$$

A is also the number of I^-_{ads} charges fixed on a single PPA after coalescence and prior to coagulation . Values $4 < A < 12$ were observed. A is most probably an integer and even due to symmetry. Higher slopes in colloid chemistry of sols are impossible. PPAs with more than 10–12 charges would be too heavy, sediment quickly and not move by brownian motion. The *DH* distances are certainly a limit of the PPA sizes. The PPA with 8 starting I^-_{ads} charges was analyzed in the present paper because r_s(PPS) = $\kappa^{-1}/2$ and r_s(PPA) = κ^{-1}. Then, the volume (PPPA) = 2^3 x volume (PPS). The third argument for selecting A=8 was the experimental observation that the slope in (32) is occasionally A=8.

DISCUSSION

The present proposal of the discrete or fixed charge potential functions in the surroundings of the coagulating PPAs should replace the double layer models based on the homogeneous distribution of the inner charges on the surface of colloidal particles. The surface is usually represented by a flat plate. The following descriptions of the homogeneous charge distribution models prove why they are inapplicable in the colloid chemistry.

The Gouy-Chapman double layer model and its theoretical potential functions were brought into the colloid chemistry from experiments performed in the system:

»polarizable (Hg) electrode/electrolyte/reference electrode«. The electromotive force (*EMF*) between the two electrodes was measured by an electrometer. It was varied by a potentiometer and obtained from a charging battery. The charge necessary to bring a Hg drop of a given size or surface to a given *EMF* was transformed into charge density (unit $\mu c/cm^2$). In this case, the inner charge on the surface is a deficit or sufficit of electrons. The counter charge is an excess of counter ions of opposite sign and is assumed to be diffuse. From the »diffuse charge density-distance function« the »Gouy-Chapman potential-distance function« was derived. It depends on the concentration of the counter ion electrolyte.

Some authors derive the surface potential using the Nernst potential equation. The Nernst potential is determined by the logarithm concentration of the PDI electrolyte. The Nernst potential is in fact the *EMF* measured by an electrometer between two electrodes: »indicator electrode/electrolyte/reference electrode«. The indicator is a second order electrode, *i.e.* a metallic electrode covered with the solid forming the colloid particles. *E.g.*, in the present case the colloid system: »$AgI/I^-_{ads}/(I^-$ electrolyte)« is equated with the system: »$Ag/AgI,I^-$ electrolyte/reference electrode«.

In fact the same cell served exclusively for determination of the I^- (Ag^+) activity. The $Ag/Ag_2S/Ag^+(I^-)$ electrode could also serve same purpose. In the determination of the H^+ adsorption on hematite or magnetite, a glass electrode can be used. There is no interconnection whatsoever between Ag_2S or glass with the colloid solid AgI or hematite, or magnetite.

It is obvious that the experimental systems used for the derivation of the Gouy-Chapman and Nernst potentials have at least three phases, while a typical colloid consists of only two phases. Neither can a Gouy-Chapman charge be formed by charging a colloid solid from an outside source, from a battery, nor can the Nernst electrode charge on a solid (*e.g.* on AgI or hematite) be formed by oxidation or reduction of the PDIs. In both cases, a reference electrode is necessary. The Nernst charge is a deficit or sufficit of electrons on the poles of the electrometer and not on solid(AgI) surface. The sign (+, 0, –) of the charge on the electrode pole depends on the reference electrode chosen while the indicator electrode potential is constant. The charge on a colloid is in fact the amount adsorbed or fixed, of PDIs (*e.g.* the amount adsorbed of I^-_{ads} on AgI or H^+ on magnetite per single particle). The equilibrium function »amount adsorbed logarithm PDI concentration« is an isotherm of the Freundlich or Langmuir type having a saturation value when the concentration of PDIs is high enough, practically when $\Delta pAg > 1$.

Some authors derive the charge density from the ratio »charge/surface area«. The charge is obtained by »fast« titration of PDIs and the surface by the Brunauer-Emmet-Teller (BET) method on the taken, dried and aged solid samples. Neither can the charge obtained by a fast titration have its equilibrium value nor can the surface of a performed dried sample remain constant after its immersion in an electrolyte, which usually causes peptization and frequently a complete dissolution followed by precipitation. The higher the concentration of the added electrolyte the higher is the adsorbed amount or the actual charge. Also, if the titration is performed by addition of the PDI electrolyte (*e.g.* Ag^+ to AgI,I^- in excess), a new surface will be formed by precipitation of the excess PDI ($I^- + Ag^+ = AgI$) and by neutralization of the adsorbed $PDI(I^-_{ads})$. It is more than certain that the charge density obtained in this way cannot represent the actual equilibrium density, neither can the plots obtained in this way represent isotherms.

Furthermore, a σ(pI) plot can be obtained solely from the experimental γ(pI) plot (13). Its first derivative reads:

$$\Sigma_0 = d\sigma/d\,pI = e_0 L \Gamma_0/S_0 MW \tag{35}$$

Here, S_0 is the specific, *i.e.* the surface per unit amount of the solid. The same (35) equation can be rewritten to read:

$$\Sigma_0 S_0 = \Gamma_0 e_0 L/MW \tag{36}$$

It follows, therefore, that for any measured Γ_0 at any given $pI_{min} < pI < pI^\circ$ an infinite number of Σ_0 and S_0 values can satisfy equation (35). Plots of the functional dependence (35) are, therefore, undefined unless S_0 and Γ_0 values are specified and unless they are measured *in situ* and their constancy proved for each set of measured function values. If these conditions are not met, any theoretical potential (Gouy-Chapman, Stern, diffuse, electrokinetic, surface, *etc.*) calculated from (35) plots without quoted Γ_0 and S_0 values remains quantitatively undetermined and physically meaningless. All theoretical calculations based on σ (log[PDI]) functions cannot be applied to colloid particles because the mass of the particles is not included.

This criticism is based on an axiomatic argument. It must be applied to all theories deriving hypothetical potentials from the calculated σ(log[PDI]) functions that were exclusively obtained from experimental γ(log[PDI]) plots. Theories of this category are especially useless if the calculated hypothetical potentials cannot be compared or checked by any experimentally measurable potentials or parameters derived from them.

Probably the latest reproduced and published experimental functions σ(pI) without the quoted Γ_0 and S_0 values were in reference 22 (Figures 1 and 9) and 23 (Figure) 1. They were used for the calculation of a series of hypothetical and, in principle, not measurable potentials.

The same criticism is applicable also to reference 25. All potential functions of the hypothetical double and triple layer structures and their uncheckable parameters, like the distance of the slipping plane and the distance of the onset of diffuse layer with the centers of the surface charge groups in the zero distance plane. If the surface charge groups are assumed to be present, then necessarily the isopotential surfaces cannot be plane, they must be curved at least in the vicinity of the same charged groups.

Also, in principle, an adsorption isotherm cannot be of the »Nernst-type«. A Nernst type, *i.e.* a logarithmic plot has no saturation value even if checked in a broad range of PDI-concentration.

It should be also noted here that in organic chemistry and biochemistry[15,16] the charges of macromolecular ions are always treated as point charges.

Equation (4) ref. 25 reads:

$$\psi_0 = \frac{RT}{F} \ln[a_{H^+}/a_H + (iep)] = \frac{RT \ln 10}{F} (pH_0 - pH) \tag{37}$$

The parameter ψ_0 is called »surface« potential and is therefore assumed to be proportional to pH without any physical explanation.

This simply means that $\psi^{o}F/RT$ is equal to the chemical potential of H^+ in the bulk electrolyte.

Equation (7) reads:

$$\psi_o = \Delta[\mu^{o}(H^+) - \mu^{o}(OH^-)]_b + \frac{RT}{2F} \ln\left(\frac{a_{H^+}}{a_{OH^-}}\right)_b \tag{38}$$

The same equation is not elementary, it can be transformed into equation (4) if one eliminates a_{OH^-} by inserting $a_{OH^-} = K^{o}_{W}/a_{H^+}$ and if one changes properly the symbols of the constant terms.

In Figure (4),[25] experimental plots of »ψ *vs.* pH« are reproduced. The ordinate parameter, ψ/mV, and the slope of the plots were calculated by speculative adjustment of seven hypothetical parameters including Hg-drop capacitance in such a way that the steepest slope became, $\Delta\, RT \ln 10/F\, \Delta$ pH $\approx$ 58 mV. The ordinate parameter ψ/mV was obtained from the variable experimental adsorbed amount of H^+ on magnetite. The variable adsorbed amount is equivalent to the variable mole fraction of H^+ in the interfacial layer. This is in contradiction with the claim on p. 114 that the »Nernst type« equation (7) can be obtained only if constant mole fraction, *i.e.* a constant adsorbed amount, is assumed. The experimental range of 3.0 < pH < 9.1 is the range of variable adsorbed amount of H^+ while the range of constant adsorbed amount would be pH < 3. Figure (4) can certainly not be accepted as an experimental proof for the correctness of the »unreasonable adjustment« of any of the »seven« (p. 124) hypothetical parameters.

The experimental equilibrium neutralization of I^-_{ads} on AgI with increase of $[Ag^+]$ was described[18,1] and a theoretical explanation by eq. (62) was proposed.[14]

The »nernstian approach«[17] is based on equilibrium distribution between the adsorbed amount and bulk concentration of PDIs. This approach is in no way connected with the Nernst potentials known in electrochemistry, where it is experimentally and theoretically well founded, while the basic principles were explained above.

The specific surface of AgI was derived[24] by comparison of slopes of the »charge density, σ, *vs. EMF*« on Hg electrode and of the slope of the function »charge density *vs.* pI RT/F log e« on aged AgI. The slope $d\sigma/d(EMF \times mW)$ on mercury was equated with slope $d\sigma/d(pI \times 58 \times mW)$ and in this way the specific surface of AgI was calculated. The Hg electrode is practically an ideal polarizable electrode. The AgI is no electrode at all.

The slope of RT/F log e of a Ag/AgI electrode is in no relation whatsoever to the colloid AgI. The physical meaning of the faraday, F, is given by the reversible amount of electricity transported through the Ag surface. Across the Hg electrode (polarizable), like the AgI surface, no electricity is passed. The comparison of the potential on a Hg electrode with pI x 58 mW in a AgI colloid system is, therefore, of no significance.

REFERENCES

1. M. Mirnik, *Croat. Chem. Acta* **42** (1970) 161.
2. M. Mirnik and S. Musić, *Progr. Colloid Polym.* Sci. **61** (1976) 36.
3. G. Gouy, *J. Chim. Phys.* **29** (1903) 145.
4. D. L. Chapman, *Phil Mag.* **25** (1913) 475.
5. D. C. Grahame, *Chem. Rev.* **P41** (1947) 441.
6. P. Delahay, *Double Layer and Electrode Kinetics*, Interscience Publishers, Inc., New York, 1865.
7. P. Debye and E. Hückel, *Z. Phys.* **24** (1923) 185.
8. H. S. Harned and B. B. Owen, *The Physical Chemistry of Electrolytic Solutions*, 3rd ed., Reinhold Pub. Comp., New York, 1958.
9. R. A. Robinson and R. H. Stokes, *Electrolyte Solutions*, 2nd ed., Butterworth's Publ. Ltd., London, 1959.
10. G. Kortüm, *Treatise on Electrochemistry*, Elsevier, Amsterdam, 1970.
11. J. O. M. Bockris and A. K. N. Reddy, *Modern Electrochemistry*, Plenum Press, New York, 1970.
12. H. R. Kruyt (Ed.), *Colloid Science*, I, Elsevier, Amsterdam, 1948.
13. M. Mirnik and K. Kvastek, *Proc. VII Int. Congr. Surf. Active Sust., Moscow*, (1976) 293.
14. M. Mirnik, *Croat. Chem. Acta* **61** (1983) 81.
15. P. Karlson, *Kurzes Lehrbuch der Biochemie*, 13. völlig neubearbeitete Aufl., G. Thieme Verl., Stuttgart, 1988.
16. A. L. Lehninger, *Biochemistry*,, 2nd ed., Worth Publ., New York, 1975.
17. M. A. Blesa and N. Kallay, *Adv. Colloid Interface Sci.* **28** (1988) 111.
18. D. Tesla-Tokmanovski, M. Herak, V. Pravdić, and M. Mirnik, *Croat. Chem. Acta* **37** (1965) 79.
19. M. Mirnik, and B. Težak, *Croat. Chem. Acta* **59** (1954) 65.
20. M. Mirnik, P. Strohal, M. Wrischer, and B, Težak, *Kolloid Z.* **160** (1958) 146.
21. M. Mirnik, *Croat. Chem. Acta* **61** (1983) 81.
22. J. Lyklema (Ed.) *Solid/Liquid Dispersions* (Tk. F. Tadros, Ed.) p. 63, Academic Press, London, 1987.
23. J. Lyklema, L. G. J. Fokkink, and A. de Keizer, *Progr. Colloid Polym. Sci.* **83** (1990) 46.
24. J. Lyklema and J. Th. G. Overbeek, *J. Colloid Sci.* **16** (1961) 595.
25. N. Kallay, R. Sprycha, M. Tomić, S. Žalac, and Ž. Torbić,*Croat. Chem. Acta* **63** (1990) 467.

LIST OF SYMBOLS

A	number of charges on PPA, slope of »log k – log *c*« plot
A, B, C, D, E, F, G, H, J	charge points on PPA
AGG	aggregate of many PPAs
c, c_a, c_c, c_0	concentration: variable, of aging, critical of coagulation, standard in I(1–1)
ccc	critical coagulation concentration ($=c_c$)
CI	counter ion
d	density, g cm^{-2}
DE	difference »kinetic – electrostatic energy«
e_0	elementary charge
EK, EW	kinetic energy, electrostatic work of PPS
EMF	electromotive force of a galvanic cell, polarization potential
h	distance in a cube
I	ionic strength
ISL	intensity of scattered light
k	Boltzmann constant
k, k_a, k_c	rate constant: variable, of aging, of coagulation
K(AgI)	ionic product of AgI
L	Avogadro-Loschmidt constant
MW	molar mass

P	number size of AGGs = number of PPAs in 1 AGG
pAg, pAg^o	= –log $[Ag^+]$, the same when $\gamma = 0$
pI, pI_{limit},	= –log $[I^-]$: variable, negative stability limit,
pI_s, pI^o	starting, when $\gamma = 0$
PPA	primary particle, many constitute 1 AGG
PPS	primary particle, stable
r_J	distance of a charge J from a point on an axis of the cube
rr	distance of the centre 0 from a point on an axis
r_s	relative radius of a PPA sphere
S_o	specific surface, m^2/g
T_A, T_B, T_C	tangents of axes O–AB/2, O–BC/2, O–C
W, W_c	stability factor: variable, in *ccc*
x, x_J	distance from the sphere surface, along an axis J
xx	preset abscissa of a charge point on the sphere surface
z, z^+, z^-	positive or negative charge number
yy	ordinate of a charge point on the sphere surface
zz	third coordinate of a charge point on the sphere surface
γ, γ_c, γ_s, γ^o	= $[I^-_{ads}]/[AgI]$: adsorbed amount of I^- per mol of precipitated AgI per dm^3 of the system: variable, in c = *ccc*, starting, standard in $c_o = I(1–1)$
Γ_o	slope of the $\gamma(\Delta pAg)$ plot
ε	permittivity of the medium
κ, κ^o	reciprocal Debye-Hückel radius of the ionic cloud, standard in $c_o = I(1–1)$
π	Ludolf's constant
ρ, ρ^o	charge density, standard (volume)
ρ_r, ρ^o_r	radial charge density standard
σ, σ^o	surface charge density, standard
Σ^o	slope of the $\sigma(EMF)$ plot
ψ_c, ψ_{DH}, ψ_{GCh}	electrostatic potentials: Coulombic, Debye-Hückel, Gouy-Chapman, ionic
ψ_{ic}, ψ^o	cloud, standard (x = 1)
ψ_{cs}, ψ_{DHs},	electrostatic potentials of 8 e_o point charges in the vicinity of the sphere
ψ_{GChs},	surface: Coulombic, Debye-Hückel, Gouy-Chapman, homogeneous electro-
ψ_{hs}, ψ_{ics}	static (no ionic cloud), ionic cloud

SAŽETAK

Potencijali primarnih sfernih čestica agregata nabijenih točkastim ili homogeno raspoređenim nabojima

M. Mirnik

Izračunani su potencijali Debye-Hückelove i Gouy-Chapmanove teorije u blizini sferne koloidne čestice koja je nabijena sa osam elementarnih naboja simetrično raspoređenih u uglove ucrtane kocke. Grafički su prikazane funkcije Coulombskoga, Debye-Hückelova, ionskog i Gouy-Chapamnova potencijala te volumne i radijalne gustoće naboja o udaljenosti, u smjeru triju karakterističnih osi kocke. Pokazan je utjecaj koncentracija iona I^- i protuiona na debljinu ionske atmosfere. Dokazuje se da je konstanta brzine koagulacije proporcionalna razlici kinetičke enegije Brownova gibanja i elektrostatskog odbijanja u momentu sraza dviju čestica okruženih ionskim oblakom. Navode se argumenti o neprimjenljivosti Nernstova i Gouy-Chapmanova potencijala u teorijama dvosloja koloidnih čestica. Svi postulati predložene teorije izvedeni su iz eksperimentalnih rezultata i zapažanja prvenstveno na koloidnom sistemu AgI. Opisan je eksperiment rasta takvih čestica prilikom dodavanja otopine Ag^+ u otopinu I^-, odnosno prilikom dodatka protuiona solu AgI.